

200-MeV- π^+ -induced single-nucleon removal from ^{24}Mg

Donald Joyce and Herbert O. Funsten
College of William and Mary, Williamsburg, Virginia 23185

B. Joseph Lieb
George Mason University, Fairfax, Virginia 22030

Hans S. Plendl and Joseph Norton
Florida State University, Tallahassee, Florida 32306

Carey E. Stronach
Virginia State University, Petersburg, Virginia 23803

V. Gordon Lind, Robert E. McAdams, and O. Harry Otteson
Utah State University, Logan, Utah 84322

L. Wayne Swenson and Chandra Pillai
Oregon State University, Corvallis, Oregon 97330

David J. Vieira
Los Alamos National Laboratory, Los Alamos, New Mexico 87545

Anthony J. Buffa
California Polytechnic State University, San Luis Obispo, California 93401
(Received 30 June 1986)

Nuclear γ rays in coincidence with outgoing pions or protons following single-nucleon removal from ^{24}Mg by 200-MeV π^+ have been detected with Ge(Li) detectors. Differential cross sections are reported for γ rays from the first excited mirror states of ^{23}Na and ^{23}Mg in coincidence with positive pions or protons detected in particle telescopes at 30° , 60° , 90° , 120° , and 150° ; angle-integrated absolute cross sections and cross section ratios $\sigma(^{23}\text{Mg})/\sigma(^{23}\text{Na})$ are calculated. These results are compared with the predictions of a Pauli-blocked plane-wave impulse approximation and the intranuclear cascade and nucleon charge exchange reaction models. The plane-wave impulse approximation and the intranuclear cascade calculations generally agree with the angular dependence of the experimental results but not the absolute magnitude. The nucleon charge exchange calculation does not reproduce the observed cross section charge ratios.

I. INTRODUCTION

The $(\pi, \pi N)$ nuclear reaction offers the potential of understanding nuclear structure and, at the same time, of studying the propagation of a strong baryon resonance, the Δ , in the nuclear medium. Before this potential can be realized, however, a better understanding of the reaction mechanism must be developed.

The $(\pi, \pi N)$ reaction has been extensively studied using two general types of experiment. In one type of experiment, the residual nucleus or specific states of the residual nucleus are identified through radiochemical techniques (e.g., Refs. 1 and 2), or via detection of prompt deexcitation γ rays (e.g., Ref. 3). Since no kinematical or angular information is obtained, these experiments integrate over both quasifree and nonquasifree components.

Interest in these experiments has centered on the charge dependence of the cross section ratios which were found to differ from the free πN ratios. For example, the cross section ratio $\sigma(\pi^+)/\sigma(\pi^-)$ for π induced neutron removal

from ^{12}C was found to have a value of 1/1.7 instead of 1/3.¹

In the other type of experiment (e.g., Refs. 4 and 5), the outgoing pion or proton is detected. With the proper geometry, the experimenter can select quasifree events; but only recently has the charged-particle energy resolution become sufficient to identify the final nuclear state. In the work of Kyle *et al.*,⁵ the π^+/π^- ratio for proton removal from ^{16}O was found to be as large as ~ 40 at forward π angles. They attributed this increase over the free πN value of 9 to a reduction in the π^-p quasifree amplitude through destructive interference with another process. They identified the interfering process as ΔN knockout.

The present study includes features of both types of experiment by detecting prompt deexcitation γ rays in coincidence with the outgoing pions or protons. It thus combines kinematic information with the ability to measure excitation of specific nuclear states.

We studied 200 MeV π^+ incident on a ^{24}Mg target.

Outgoing charged particles (scattered π^+ and knocked out protons) were detected by scintillator telescopes at 30° , 60° , 90° , 120° , and 150° and identified by their dE/dX . Coincident nuclear γ rays were detected in one of two Ge(Li) detectors and identified by their energy. One can thus study several different $(\pi, \pi N)$ reaction channels. For example, ^{23}Na γ rays in coincidence with a π^+ or a p can result only from a direct proton knockout with no charge exchange. ^{23}Mg γ rays in coincidence with a π^+ can result only from a direct neutron knockout. On the other hand, ^{23}Mg γ rays in coincidence with a proton can only result from a charge exchange reaction.

^{24}Mg was chosen as a target because single nucleon removal from ^{24}Mg results in mirror nuclei ^{23}Mg and ^{23}Na . This provides a test of both single proton and single neutron removal mechanisms with pions. Furthermore, the single nucleon removal spectroscopic strengths ($1d_{5/2}$ and $1p_{1/2}$) for ^{23}Na and ^{23}Mg from ^{24}Mg are concentrated in two low-lying excited states which γ decay directly to the ground state.⁶ For both ^{23}Na and ^{23}Mg , the first excited states (≈ 0.45 MeV, $\frac{1}{2}^+$) have spectroscopic factors of ~ 4 to 6, and the $\frac{1}{2}^-$ excited states (at 2.64 MeV in ^{23}Na and at 2.77 MeV in ^{23}Mg) have spectroscopic factors of ≈ 4 as determined from the analysis of single-nucleon removal reactions on ^{24}Mg .⁶ This yields for the $\frac{1}{2}^+$ levels an occupation number $C^2S \approx 2$, one-half the $1d_{5/2}$ shell limit of 4 in ^{24}Mg . [C is the isospin coupling coefficient, $(T_f T_f | 1/2 \tau_N | T_i \tau_i) = \sqrt{1/2}$.] Other bound excited states have considerably smaller spectroscopic factors. They predominantly feed the first excited state, but the combined effect of this γ -ray feeding should be less than $\approx 25\%$ of the overall strength of the first excited state if all states were populated in proportion to their spectroscopic factors.

The suitability of a ^{24}Mg target for $(\pi, \pi N)$ reaction work was established previously by the results of an inclusive study of γ rays from π reactions on ^{24}Mg .³ The two above-mentioned states in ^{23}Na and ^{23}Mg with large spectroscopic factors were strongly excited; there was no evidence for background γ rays that might overlap these states. Another reason for the selection of a ^{24}Mg target was its suitability for a parallel study⁷ of the angular correlation of γ rays from (π, π') scattering.

A feasibility study of the techniques employed in this work was undertaken at LAMPF using a single gamma-ray detector in coincidence with a single charged particle telescope.⁸ The results of that study suggested the need to develop a large-scale coincidence measurement system sensitive to deexcitation gamma rays, knockout nucleons, and scattered pions. Such an improved system was developed and used in the present work.

II. EXPERIMENTAL APPARATUS AND PROCEDURES

The experiment was performed with a 200 MeV π^+ beam from the high-energy pion channel (P^3) of LAMPF. This beam had a contamination of 6.6% μ^+ and 2.0% e^+ . The beam spot size was typically 2.5 cm in diameter; the muon halo was 7 cm. The momentum resolution was $\approx 0.5\%$. The target consisted of natural magnesium met-

al (79% ^{24}Mg) with an average thickness of 0.57 ± 0.02 g/cm².

The experimental geometry was defined by six scintillation telescopes for charged particle detection and two Ge(Li) spectrometers to detect γ rays (see Fig. 1). Each of the six particle telescopes consisted of six NE102 scintillators. They were, solid angle defining Ω , energy loss Δ , and energy E , in addition to rear, left-side veto, and right-side veto scintillators. Each scintillator was coupled to a 5 cm photomultiplier tube, except for the E scintillator, which was coupled to two 12.5 cm photomultiplier tubes, one at each end. The detector thicknesses were 0.160 cm (Ω), 0.320 cm (Δ), 0.635 cm (vetos and rear scintillators), and 15.75 cm (E). The dimensions of each telescope component were the same for each telescope with the exception of the Ω scintillators. The Ω scintillators for telescopes 1, 5, and 6 at $\pm 30^\circ$ and 150° had to be moved further from the target to avoid the beam halo; they were made correspondingly larger so that all the telescopes subtended the same solid angle.

The Ω and Δ counters together defined the solid angle (~ 0.18 sr) of each telescope, and the E scintillator determined the particle energy. All three scintillators were used for particle identification. The rear scintillator tagged particles which had not stopped in the previous scintillators. The two side veto scintillators tagged particles scattering out of or into sides of the E scintillators. During off-line data analysis, however, this feature was not used. Calculation of the telescope solid angles was performed following the method of Gotch and Yogi,⁹ considering the size and location of the Ω , Δ , and E scintillators for each telescope. All telescopes except number 6 were mounted together on a pivoting table with their axis

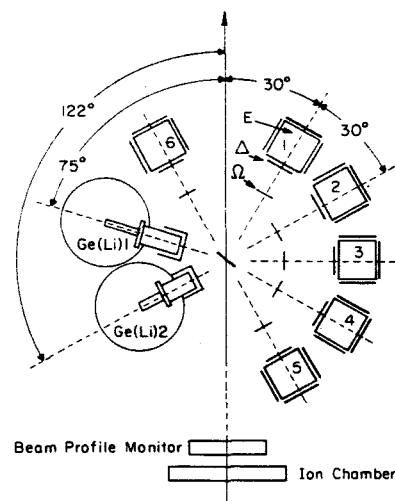


FIG. 1. Experimental geometry. The rear and side veto counters surrounding each E counter are shown but not labeled.

directly under the target centerline. Telescope 6 was mounted on a similar but smaller table pivoting on the same axis.

Two Ge(Li) γ ray spectrometers were used in the present experiment, an Ortec 9% efficient and a Princeton Gamma-Tech 11% efficient detector. Both detectors were fitted with NE102 anticoincidence scintillator cups to tag charged particles entering them. They were mounted on one rolling table to facilitate positioning and shielding. One detector was located at -75° and the other at -122° relative to the pion beam line axis (see Fig. 1). Additional experimental details are given in Ref. 7.

The beam intensity was monitored with a 7.6 cm thick ion chamber filled with argon, and the beam profile was monitored with a LAMPF wire chamber system.¹⁰ The absolute cross sections were normalized to the differential inelastic π scattering cross sections from the 2^+ state of ^{24}Mg .¹¹

The six telescopes were calibrated in energy by tuning the channel for low-intensity protons at 50, 133, and 191 MeV and placing each of the telescopes in the beam. The telescopes were also calibrated with the pion and proton quasielastic scattering peaks from the experimental runs as well as with the maximum energy deposited in the E scintillators for pions and protons. The telescope calibration runs were also used to determine the efficiencies of the six telescopes. They were found to average $(96 \pm 2)\%$.

The energy responses of the two Ge(Li) detectors were periodically calibrated by placing ^{228}Th , ^{54}Mn , and ^{137}Cs sources at the target location. Well-known strong γ -ray peaks in the experimental data provided additional energy calibration, including the ^{24}Mg and ^{23}Na first excited state to ground transitions. The maximum deviation of the calibration data from a linear fit was 0.7 keV. Relative and absolute Ge(Li) detector efficiencies were also determined in the source calibration runs.

A valid data event consisted of a coincidence between a particle telescope signal and a Ge(Li) γ ray. For each event, pulse heights were digitized for Ω , Δ , E (two photomultipliers), and rear scintillators as well as the Ge(Li) detectors. All data were read into a PDP-11 computer and written on magnetic tape for later replay.

Particles were identified from their Δ and E pulse heights using the method of Goulding *et al.*¹² A particle which passed completely through the E scintillator (75 MeV pions and 160 MeV protons) as indicated by the rear scintillator was treated using the method of England.¹³ Figure 2 shows a typical dE/dx vs E dot plot (for Telescope 1, 30°), with the pions and protons identified.

Statistics were not sufficient to allow cuts on pion or proton energy. Figure 3 shows the spectrum in the Ge(Li) detector at 75° in coincidence with a pion or a proton in any one of the six telescopes. Figure 4 shows the random (off timing peak) spectrum for this detector.

The γ rays in these spectra were identified by their energy, and areas were determined by summing channels and subtracting background. Cross sections were calculated from the relative areas and from the Ge(Li) and the particle telescope efficiencies. As noted above, the cross sections were normalized to the ^{24}Mg 2^+ differential inelastic scattering cross sections of Bolger.¹¹ Major sources

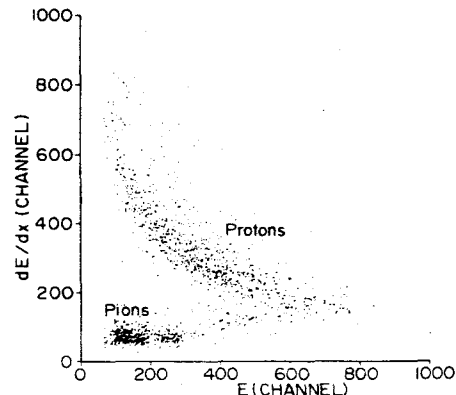


FIG. 2. A dE/dx vs E dot plot for telescope 1 at 30° . The E signal was from one of the two photomultipliers of that scintillator.

of error were the following: statistical errors, errors in the absolute normalization to the inelastic data ($\approx 15\%$), Ge(Li) efficiency calibration ($\approx 9\%$), and telescope solid angle determination ($\approx 6\%$).

In addition to the strong first excited 2^+ states at 0.439 MeV in ^{23}Na and 0.450 MeV in ^{23}Mg (see Fig. 3), there was evidence for the fourth excited $\frac{7}{2}^-$ state in ^{23}Na at 2.64 MeV, but its Doppler-broadened width prevented a differential cross section measurement. There was no sign of its mirror state in ^{23}Mg .

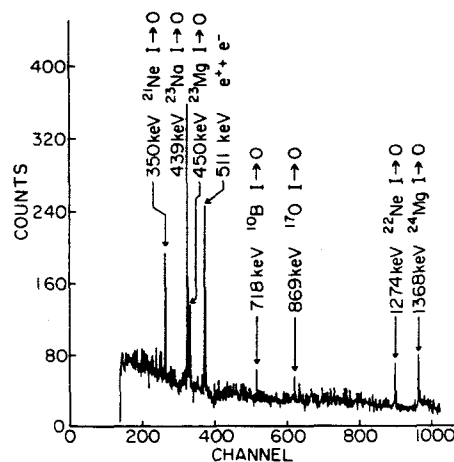


FIG. 3. Ge(Li) 1γ -ray spectrum in coincidence with a π^+ or p from $^{24}\text{Mg}(\pi^+, \pi N)$ in any one of the six particle telescopes (low-energy portion).

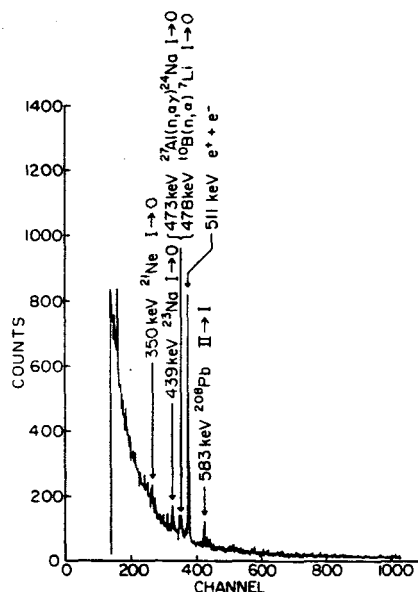


FIG. 4. Ge(Li) 1 γ -ray spectrum in random coincidence (low-energy portion).

III. COMPARISON OF ANGULAR DISTRIBUTIONS WITH REACTION MODELS

The experimental differential cross sections for production of the 0.439 and 0.450 MeV γ rays in coincidence with outgoing pions or protons are listed in Table I for the two Ge(Li) detectors. The averages (last column of Table I) were calculated using the inverse of the fractional errors as weights. Where two cross sections differed greatly, the errors were increased in order to be more conservative. Data from telescopes 1 and 6 were averaged to give one data point at 30° .

The cross sections were extracted from the data by assuming isotropic γ ray correlation with the outgoing pion or proton. This assumption would be rigorously true for direct plane wave nucleon knockout and can be seen to be approximately true within experimental uncertainties by comparing the relative cross sections of Ge(Li) 1 and 2 listed in columns 4 and 5 of Table I. [Ge(Li) 1 and 2 had an angular separation of 50° .] This absence of angular correlation is in contrast to the expected strong $\sin^2 2\theta_{\gamma q}$ correlation that was observed in this experiment for inelastic π^+ scattering to the 1.37 MeV first excited state of ^{24}Mg .⁷ ($\theta_{\gamma q}$ is the angle between the γ ray and the inelastic momentum transfer direction.)

Proton and pion differential cross sections were compared with predictions of an intranuclear cascade (INC) code developed by Fraenkel *et al.*¹⁴ and with the predictions of a simple plane-wave impulse approximation (PWIA) which assumes only a single collision of the incident pion with a nucleon. In Sec. IV, cross section

charge ratios are compared with these models and also with a model that assumes final-state nucleon charge exchange (NCX).¹⁵

The INC predictions were based on 5×10^4 cascades of 200 MeV π^+ on ^{24}Mg . The code has no free parameters. The program output was sorted to yield differential π^+ and proton cross sections at the angles measured in the present experiment for events in which the final nucleus was ^{23}Na or ^{23}Mg in a bound state. Since only single nucleon emission was involved, that part of the code that evaluates evaporation subsequent to the cascade was not used. A ^{23}Na or ^{23}Mg nucleus was assumed to retain its identity if its excitation energy calculated by INC following the cascade was less than its known particle stability energy. Since the INC code does not include details of nuclear structure or predict specific nuclear states calculated contributions to the $^{23}\text{Na}/^{23}\text{Mg}$ bound states arose from the entire nuclear volume and not just from the nuclear surface (i.e., $1d_{5/2}$ shell nucleons). Hence the results were multiplied by the ratio

$$r = \frac{\sum_{J^P} S^-(J^P) F(J^P, \frac{1}{2}^+)}{\sum_{J^P} S^-(J^P)},$$

where $S^-(J^P)$ is the spectroscopic factor for neutron or proton removal to a ^{23}Na or ^{23}Mg bound state of spin parity J^P and $F(J^P, \frac{1}{2}^+)$ is the relative fraction of γ feeding from an initial J^P state down to the $\frac{1}{2}^+$ first excited state. The sum is taken over all bound levels using spectroscopic factors and γ branching ratios from Ref. 6; $r \approx 0.6$ for both ^{23}Na and ^{23}Mg . The INC results quoted in the present paper have been reduced by this factor.

The INC calculation showed that a large fraction ($\approx 90\%$) of production of a bound state of the $A-1$ residual nuclei results from a single collision of the incident pion on a nucleon with no further interaction. Furthermore, in the calculation the probability of the residual nucleus being left with a given excitation decreased monotonically with increasing excitation energy.

The PWIA predictions for the cross sections were calculated using the semiempirical free πN phase shifts of Rowe *et al.*¹⁶ The resulting cross sections were reduced, at small pion scattering angles, by Pauli blocking using a degenerate Fermi sphere uniformly filled up to a momentum of $k_F = 270$ MeV/c. The Pauli blocking was calculated from the quantity $(V-N)/V$, where N is the phase space volume common to the Fermi sphere and a similar Fermi sphere whose center is displaced by the free πN scattering momentum transfer to the nucleon, $q = 2k_\pi \sin \theta_\pi / 2$. V is the sphere's volume. This caused the resulting cross section at $\theta_\pi = 0^\circ$ to be 0 and at $\theta_\pi \sim 80^\circ$ to approach the free $\pi\text{-N}$ cross section. This cross section was then multiplied by the $1d_{5/2}$ proton or neutron occupation number for the first excited state, $C^2S_{\bar{N}} = 2.2$ defined above. It was necessary to additionally scale the resulting PWIA prediction to the data by multiplying by factors of $\sim \frac{1}{3}$ to $\frac{1}{5}$. This indicates the predominance of other processes such as pion absorption and secondary scatterings.

The PWIA calculation was performed only to estimate the trends of the experimental data. It, however, demon-

TABLE I. Experimental differential cross sections for $^{24}\text{Mg}(\pi, \pi N)$. $\sigma_{\pi}(^{23}\text{Na})$ is the differential cross section for production of the ^{23}Na first excited state ($\frac{5}{2}^+$, 0.439 MeV) in coincidence with a π^+ . Similar definitions apply for the other cross sections. Results are shown for each Ge(Li) detector and as an average which was weighted by the fractional errors. Telescope 1 was averaged with telescope 6 for the 30° results.

Reaction	Telescope	Angle (deg)	Ge(Li) 1 (mb/sr)	Ge(Li) 2 (mb/sr)	Average (mb/sr)
$\sigma_{\pi}(^{23}\text{Na})$	1	30	7.3 \pm 1.9	4.6 \pm 1.2	5.2 \pm 1.1
	6	30	4.8 \pm 1.3	1.9 \pm 1.3	
	2	60	4.4 \pm 1.2	3.3 \pm 0.9	3.9 \pm 0.9
	3	90	4.0 \pm 1.1	1.6 \pm 0.5	3.0 \pm 1.0
	4	120	6.3 \pm 1.7	4.1 \pm 1.1	5.2 \pm 1.0
$\sigma_{\pi}(^{23}\text{Mg})$	5	150	6.2 \pm 1.6	4.2 \pm 1.1	5.2 \pm 1.0
	1	30	1.5 \pm 0.5	1.9 \pm 0.5	1.4 \pm 0.5
	6	30	1.4 \pm 0.5	0.31 \pm 0.15	
	2	60	1.1 \pm 0.4	0.74 \pm 0.25	0.90 \pm 0.22
	3	90	0.82 \pm 0.34	0.97 \pm 0.30	0.92 \pm 0.23
$\sigma_p(^{23}\text{Na})$	4	120	1.2 \pm 0.5	0.89 \pm 0.29	1.0 \pm 0.25
	5	150	0.72 \pm 0.28	1.3 \pm 0.4	1.1 \pm 0.30
	1	30	15.0 \pm 4.0	16.0 \pm 4.0	15.0 \pm 4.0
	6	30	18.0 \pm 4.0	11.0 \pm 3.0	
	2	60	4.8 \pm 1.3	4.0 \pm 1.1	4.4 \pm 0.9
$\sigma_p(^{23}\text{Mg})$	3	90	0.59 \pm 0.28	0.85 \pm 0.30	0.76 \pm 0.20
	4	120	1.5 \pm 0.5	0.87 \pm 0.31	1.2 \pm 0.3
	5	150	1.3 \pm 0.5	0.45 \pm 0.20	0.93 \pm 0.27
	1	30	7.6 \pm 2.0	7.7 \pm 1.9	5.8 \pm 1.4
	6	30	5.1 \pm 1.4	2.8 \pm 0.80	
$\sigma_p(^{24}\text{Mg})$	2	60	2.1 \pm 0.7	1.3 \pm 0.4	1.7 \pm 0.4
	3	90	0.48 \pm 0.24	0.31 \pm 0.15	0.39 \pm 0.14
	4	120	0.45 \pm 0.25	0.59 \pm 0.25	0.54 \pm 0.18
	5	150	0.93 \pm 0.38	0.28 \pm 0.15	0.69 \pm 0.22

states the role of Pauli blocking in reducing the forward angle pion scattering from the free πN .

A. Pion angular distributions

Figure 5 shows experimental and calculated angular distributions for outgoing pions that are in coincidence with γ rays from the first excited states of ^{23}Mg and ^{23}Na . The solid curve represents the Pauli-blocked PWIA results described above; the open circles are the results from the INC calculation. Without Pauli blocking, the pion differential cross section would rise steadily as θ_{π} decreases below $\sim 60^\circ$. At $\theta_{\pi} = 30^\circ$, the PWIA cross section is reduced by a factor of ~ 2 relative to the free case. Both INC and PWIA calculations (and the data) display Pauli blocking with decreasing θ_{π} ; the INC cross section falls off more rapidly than the PWIA cross section. An effect that could account for this discrepancy is nuclear shadowing of forward-scattered pions for the INC calculation. In the PWIA calculation, this effect has not been included.

B. Proton angular distributions

Figure 6 displays the experimental angular distributions for outgoing protons in coincidence with γ rays from the

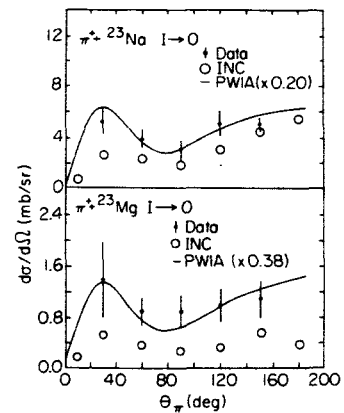


FIG. 5. Differential cross sections of outgoing π^+ from $^{24}\text{Mg}(\pi^+, \pi^+ N)$ in coincidence with γ rays from the first excited states of ^{23}Na and ^{23}Mg compared with Pauli-blocked plane-wave impulse approximation (PWIA) and intranuclear cascade (INC) calculations. PWIA values have been multiplied by 0.20 for ^{23}Na and by 0.38 for ^{23}Mg .

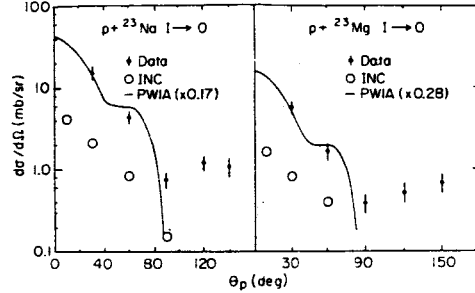


FIG. 6. Differential cross sections of protons from $^{24}\text{Mg}(\pi^+, p)$ in coincidence with γ rays from the first excited states of ^{23}Na and ^{23}Mg compared with Pauli-blocked plane-wave impulse (PWIA) and intranuclear cascade (INC) calculations. PWIA values have been multiplied by 0.17 for ^{23}Na and by 0.28 for ^{23}Mg . PWIA and INC values at backward angles are < 0.1 mb/sr and hence do not show up on the semilogarithmic plot.

first excited states of ^{23}Mg and ^{23}Na , together with PWIA and INC results (solid curves and open circles, respectively). The angular distributions have the general shape of free π -N scattering, in which case no protons would be emitted at angles greater than 90° .

The E scintillator thickness (15 g/cm^2) was insufficient to permit derivation of pion energy spectra, but was adequate for determination of proton energy spectra by use of a foldback procedure.⁷ The 30° and 60° γ -coincident proton spectra are shown in Fig. 7. The arrows indicate the energies for free π N scattering; the dashed lines indicate the INC results. Coincident proton spectra for $\theta_p \geq 90^\circ$ had few total counts; as expected, no peak was observed. The apparent differences between the 60° spectra and the INC predictions may be instrumental: the steep left-hand shoulder is due to electronic low-energy cutoff, and the high-energy tail is partially due to scintillator energy resolution. The cross sections at 60° were corrected for the low-energy cutoff.

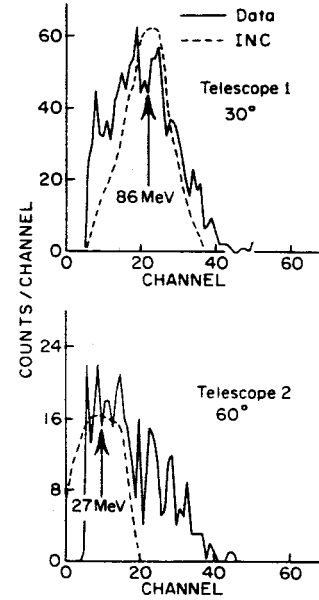


FIG. 7. Energy spectra of protons from $^{24}\text{Mg}(\pi^+, p)$ detected at 30° and 60° in coincidence with γ rays from the first excited states of ^{23}Na and ^{23}Mg compared with INC calculations (dashed line). The arrows indicate the energies for free π N scattering.

IV. DISCUSSION

The experimental angle-integrated absolute cross sections listed in Table II are $\sim \frac{1}{3}$ to $\sim \frac{1}{5}$ of those predicted by the PWIA as discussed above. They are, however, 3 times greater than those predicted by INC. Particularly at the Δ resonance energy, the assumption of a quasifree π N interaction which is implicit in both PWIA and INC is questionable. The 200 mb free π N cross section at the resonance yields a spatial width of $\sim 5 \text{ fm}$ resulting in a

TABLE II. Experimental and calculated angle-integrated absolute cross sections for $^{24}\text{Mg}(\pi^+, \pi N)^{23}\text{Mg}(\frac{5}{2}^+, 0.450 \text{ MeV})$ and $^{24}\text{Mg}(\pi^+, \pi^+ p)^{23}\text{Na}(\frac{5}{2}^+, 0.439 \text{ MeV})$. σ_{PWIA} was calculated assuming nuclear Pauli blocking and nucleon occupation numbers given by C^{2S-} (see text).

Final nucleus	Outgoing particle	σ_{exp} (mb)	σ_{INC} (mb)	$\frac{\sigma_{\text{exp}}}{\sigma_{\text{INC}}}$	σ_{PWIA} (mb)	$\frac{\sigma_{\text{exp}}}{\sigma_{\text{PWIA}}}$
^{23}Na	π^+	52 ± 9	19	2.7	263	0.20
	p	44 ± 9	20	2.2	263	0.17
^{23}Mg	π^+	11 ± 2	2.7	4.1	29	0.38
	p	16 ± 3	3.9	4.1	58	0.28

"swelling" of the nucleon-pion system to a size encompassing up to two adjacent nucleons. This "swelling" yields total π -nucleus cross sections that are typically twice the nuclear geometrical cross section. For example, in ^{27}Al , the geometrical cross section is ~ 450 mb, whereas the total pion cross section is ~ 960 mb (Ref. 16) and is divided approximately equally among pion capture, nuclear elastic, and nonelastic processes. The cross sections that remain for production of states observed in the present experiment are thus a small fraction of the total cross sections. Hence they would be sensitive to variations in any of the above components.

The ratios $\sigma_{\pi}(^{23}\text{Na})/\sigma_{\pi}(^{23}\text{Mg})$ for the π^+ coincident differential cross sections have values of ~ 4 , approximately independent of θ_{π} (see Table I). This is in disagreement with the results of Kyle *et al.*⁵ at $T_{\pi}=240$ MeV in which the corresponding charge ratio $R=\sigma(\pi^+)/\sigma(\pi^-)$ for $^{16}\text{O}(\pi^{\pm},\pi^{\pm}p)^{15}\text{N}_{g.s.}$ reaches a very large value, $R \geq 30$, for forward angles, $\theta_{\pi} \leq 35^\circ$. Kyle *et al.* suggest that this enhancement over the quasifree value of 9 comes from a reduction in the π^-p cross section, as π^+p enhancement is unlikely. In our experiment, however, the angle-integrated π^+ coincident ^{23}Mg $\frac{5}{2}^+$ cross section, which corresponds to the π^- cross section of Kyle *et al.*, is relative to PWIA, the largest of all four measured cross sections (see Table II, column 7). It may be noted that the enhancement found by Kyle *et al.* occurs at scattering angles where Pauli blocking is predominant.

Our π^+ and p coincident ^{23}Na cross sections are in agreement with equivalent cross sections obtained from $^{12}\text{C}(\pi^+, \pi^+p)$ data of Piasetzky *et al.*,⁴ who used a double arm spectrometer system. Their cross section values approximately equal those for free π^+p scattering; and assuming that four p shell protons are available, their effective participation ratio is approximately 0.25, which agrees with our results for ^{23}Na (Table II, column 7). However, their $^{12}\text{C}(\pi^-, \pi^-p)$ cross section is $\sim 60\%$ greater than our equivalent π^+ coincident ^{23}Mg cross section.

As mentioned above, the INC predictions fall below the experimental results by a factor of $\approx \frac{1}{3}$. An examination of the particle histories generated by the INC code yields the following further information on the $^{24}\text{Mg}(\pi, \pi p)$ reaction:

(A) INC predicts total, elastic, and absorption cross sections of 980, 400, and 230 mb, respectively, in agreement with 960, 380 and 218 mb, as measured by Ashery *et al.*¹⁷ for 245 MeV $\pi^+ + ^{27}\text{Al}$.

(B) INC indicates that 75% of the Δ 's decay before striking a nucleon. This is due to the short free decay length of the Δ (~ 0.4 fm) and is consistent with the PWIA calculation which indicates that only $\sim \frac{1}{3}$ of the Δ decays are Pauli blocked.

(C) According to the INC results, pions from Δ decay predominately do not escape the nucleus; 75% of the pions from Δ decay strike a nucleon to reform another Δ . Using the Δ decay probability given above in (B), this yields an average of two sequential Δ 's formed for each incident $T_{\pi}=200$ MeV pion on the nucleus. In a single scattering, the pion loses an average of 60 MeV lab kinetic energy; after two or more pion scatterings through Δ for-

mation, T_{π} will have dropped considerably below resonance energy. INC yields a pion scattering mean free path λ_{π} of 1.2 fm; cf. $\lambda_{\pi}=1/(\rho\sigma_{\pi})_{\text{total}} \approx 2.3$ fm. (Pion absorption occurs only through $\Delta N \rightarrow NN$.)

(D) INC indicates that approximately 70% of the protons resulting from Δ decay escape the nucleus without further scattering. INC yields $\lambda_p=4.5$ fm; this is in agreement with $\lambda_p=1/\rho\sigma_p > 5$ fm obtained from free, but Pauli blocked¹⁸ NN total cross sections¹⁹ and a ^{24}Mg uniform nuclear matter density ρ calculated using a radius parameter of 1.315 fm.²⁰ The INC result is also in agreement with estimates by Schiffer.²¹ Of the scattered Δ decay protons, approximately half undergo charge exchange before escaping in the INC calculations. Since only 30% of the protons do not escape, this yields a probability for NCX of only $\approx 15\%$.

(E) Approximately 40% of the total cross section for incident pions results in pion capture ($\Delta N \rightarrow NN$), according to the INC calculation. Measurements by Ashery *et al.*¹⁷ indicate a ratio of capture-to-total cross section of $\approx 30\%$.

The INC results discussed above suggest that pion multiple scattering, occurring mainly by sequential Δ production and decay, is a predominant process, being more important ($\lambda_{\pi}=1.2$ fm) than nucleon multiple scattering ($\lambda_p \approx 5$ fm), which was proposed some time ago¹⁵ as a major process in pion-induced nucleon knockout at Δ resonance energies. In the latter process the nucleon from Δ decay undergoes subsequent incoherent nuclear scattering with a probability of nucleon charge exchange (NCX), $P \approx 0.1 \rightarrow 0.2$,¹⁵ as determined from cross section ratios obtained in $\sigma[^{12}\text{C}(\pi^+, x)^{11}\text{C}]/\sigma[^{12}\text{C}(\pi^-, x)^{11}\text{C}]$ activation experiments.¹ In the present experiment, both π^+ and p coincident cross sections for deexcitation γ rays are determined. Hence the present experiment provides a more sensitive test of the NCX model than the previous activation experiments, which sum over these two final states.

The NCX calculation predicts cross sections for the final states $^{23}\text{Mg} + \pi^+$, $^{23}\text{Mg} + p$, $^{23}\text{Na} + \pi^+$, and $^{23}\text{Na} + p$ to be in the ratio of $(1+9P):2:(9+P):(9+P)$. Since the ^{23}Na residual nucleus must be accompanied by both π^+ and p , the final states $^{23}\text{Na} + \pi^+$ and $^{23}\text{Na} + p$ must have the same cross sections regardless of the reaction model. Hence, the two experimental ^{23}Na cross sections (see Table II) were averaged, yielding $\sigma[^{23}\text{Na}(\text{av})]=48 \pm 8$ mb. There are then only two independent cross section ratios. Let them be the ratios of $\sigma[^{23}\text{Mg} + \pi^+]$ and $\sigma[^{23}\text{Mg} + p]$ to $\sigma[^{23}\text{Na}(\text{av})]$. The first ratio,

$$R_1 = \sigma[^{23}\text{Mg} + \pi^+]/\sigma[^{23}\text{Na}(\text{av})] = 0.23 \pm 0.04,$$

yields $P \approx 0.12 \pm 0.04$, consistent with values of P obtained from activation work. (Quasifree $R_1=1/9$.) However, the second ratio, obtained from the proton component of the ^{23}Mg final state, has a value

$$R_2 = \sigma[^{23}\text{Mg} + p]/\sigma[^{23}\text{Na}(\text{av})] \approx 0.33 \pm 0.05,$$

yielding a negative value of P , -2.9 ± 0.9 , which is inconsistent with NCX, even though the uncertainty is quite large. (Quasifree $R_2=2/9$.) Because of electronic cutoff and the lack of scintillators in the forward direction where

the proton cross section peaks, we may be undercounting proton events and hence R_2 . However, an increase in R_2 would worsen agreement with NCX.

A comparison of our experimental results with the results of activation measurements can be made by summing the measured π^+ and p components of the ^{23}Mg cross section (see Table II). This yields a ratio of

$$\sigma[(^{23}\text{Mg} + \pi^+) + (^{23}\text{Mg} + p)] / \sigma[^{23}\text{Na}(av)] \approx 0.56 \pm 0.06,$$

which, in turn, yields a value of $P \approx 0.24 \pm 0.07$, consistent with the value of P obtained from activation measurements.

The above results indicate that whereas the NCX model can explain inclusive cross section results like those obtained by activation measurements, it is inconsistent with the more exclusive cross sections obtained in the present experiment. In a recent paper, Ohkubo and Liu²² include the effects of quantum mechanical interference between quasifree and nonquasifree (NCX and π charge exchange) reaction processes using distorted waves. Their calculations result in significantly better agreement with the experimental results for $^{12}\text{C}(\pi^+, \pi\text{N})^{11}\text{C}$ cross section ratios¹ than the previously incoherent NCX calculations.¹⁵ In a subsequent paper Ohkubo *et al.*² conclude that both NCX and the interference effects decrease considerably in magnitude as the target mass is increased from $A=12$. Their results suggest that these effects are small for an $A=24$ target. Hence these predictions and the results of the present experiment are in disagreement with the NCX model (PWIA predicts $P=0$, in clear disagreement with all data).

A two baryon process in which an initial Δ subsequently interacts with a nucleon in a $(\Delta\text{N})_{T=2}$ state can, by itself, reproduce measured values of R_1 and R_2 . Such a process, in which one of the $(\Delta\text{N})_{T=2}$ decay nucleons subsequently remains in the nucleus, yields $R_1=0.22$, $R_2=0.37$, i.e., values close to those observed. Although there has been evidence for a possible $(\Delta\text{N})_{T=2}$ attractive potential,²³ an examination of the magnitude of pion double charge exchange cross sections casts doubt on this process. Even after allowing for the isospin recoupling, which yields for pion double charge exchange a $(\Delta\text{N})_{T=2}$ component $\sim \frac{1}{3}$, any ΔN contribution that is sufficiently large to yield a reasonable $(\pi, \pi\text{N})$ reaction would result in

a pion double charge exchange cross section too high by at least a factor of 10.

V. CONCLUSION

The experimentally determined pion and proton differential cross sections for deexcitation γ rays from the $\frac{1}{2}^+$ first excited states of ^{23}Na and ^{23}Mg in coincidence with outgoing π^+ or p from $^{24}\text{Mg}(\pi^+, \pi\text{N})$ have been measured and compared with the results of calculations based on several $(\pi, \pi\text{N})$ reaction models, in particular on a Pauli blocked plane-wave impulse approximation (PWIA), on intranuclear cascade (INC) models, and on charge exchange of the outgoing nucleon (NCX).

Both the PWIA and the INC calculations reproduce the approximate shape of the observed π^+ and p angular distributions, but not the magnitude. The PWIA calculation, which was done primarily to illustrate the trends in the data, resulted in cross sections that were a factor of ~ 3 to 5 too large. On the other hand, the INC calculations, which can be considered absolute, were a factor of ~ 3 too small. These calculations indicate that rescattering of the outgoing pions is a more important process than rescattering of the outgoing nucleons. The NCX model is put to a more sensitive test by the present experiment than by previous activation experiments, since π^+ and p coincident cross section ratios for deexcitation γ rays are determined separately rather than together. The NCX results are inconsistent with our experimental results.

These comparisons suggest that a more detailed description of the πN interaction in a nucleus, such as the Δ -hole model of Hirata, Lenz and Theis,²⁴ may be needed for a better understanding of the processes involved in the $(\pi, \pi\text{N})$ reaction.

ACKNOWLEDGMENTS

We wish to thank Jean Julien, Herbert O. Funsten III, and David C. Plendl for their participation in the data collection, Peter Gram for valuable discussion on experimental details, and Robert Damjanovich and other members of the LAMPF staff for technical assistance. This work was supported in part by the NSF; the participation of one of us (C.E.S.) was also supported in part by NASA.

¹B. J. Dropesky, G. W. Butler, C. J. Orth, R. A. Williams, M. A. Yates-Williams, G. Friedlander and S. B. Kaufman, Phys. Rev. C **20**, 1844 (1979); L. H. Batist, V. D. Vitman, V. P. Koptev, M. M. Makarov, A. A. Naberezhnov, V. V. Nelyubin, G. Z. Obrant, V. V. Sarantsev and G. V. Scherbakov, Nucl. Phys. A **254**, 480 (1975).

²Y. Ohkubo, C. J. Orth, D. J. Vieira, and L. C. Liu, Phys. Rev. C **31**, 510 (1985).

³B. J. Lieb, H. S. Plendl, C. E. Stronach, H. O. Funsten, and V. G. Lind, Phys. Rev. C **19**, 2405 (1979).

⁴E. Piasetzky, D. Ashery, A. Altman, A. J. Yavin, F. W. Schlepütz, R. J. Powers, W. Bertl, L. Felawka, H. K. Walter,

R. G. Winter, and J. Van Der Pluym, Phys. Rev. C **25**, 2687 (1982).

⁵G. S. Kyle, P. A. Amandruz, T. S. Bauer, J. J. Domingo, C. H. Q. Ingram, J. Jansen, D. Renker, J. Zichy, R. Stamminger, and F. Vogler, Phys. Rev. Lett. **52**, 974 (1984).

⁶P. M. Endt and C. Van der Leun, Nucl. Phys. A **310**, (1978).

⁷D. Joyce, Ph.D. thesis, College of William and Mary, 1982.

⁸V. G. Lind, R. E. McAdams, O. H. Otteson, W. F. Denig, C. A. Goulding, M. Greenfield, H. S. Plendl, B. J. Lieb, C. E. Stronach, P. A. M. Gram, and T. Sharma, Phys. Rev. Lett. **41**, 1023 (1978).

⁹H. Gotch and H. Yogi, Nucl. Instrum. Methods **96**, 45 (1971).

- ¹⁰G. J. Krause and P. A. M. Gram, LASL Report No. LA-7142, 1978 (unpublished).
- ¹¹J. Bolger, private communication.
- ¹²F. S. Goulding, D. A. Landis, J. Cerny, and R. H. Pehl, Nucl. Instrum. Methods 31, 1 (1964).
- ¹³J. B. A. England, *Techniques in Nuclear Structure Physics* (Wiley, New York, 1974), Pt. 2, p. 419.
- ¹⁴Z. Fraenkel, Phys. Rev. 130, 2407 (1963); G. D. Harp, K. Chen, G. Friedlander, Z. Fraenkel, and J. M. Miller, Phys. Rev. C 8, 581 (1973).
- ¹⁵M. M. Sternheim and R. R. Silbar, Phys. Rev. Lett. 34, 824 (1975).
- ¹⁶G. Rowe, M. Salomon, and R. H. Landau, Phys. Rev. C 18, 584 (1978).
- ¹⁷D. Ashery, I. Navon, G. Azuelos, H. J. Pfeiffer, H. K. Walter, and F. W. Schlegel, Phys. Rev. C 23, 2173 (1981).
- ¹⁸K. Nishijima, *Fundamental Particles* (Benjamin, Reading, 1963), p. 98.
- ¹⁹W. N. Hess, Rev. Mod. Phys. 30, 368 (1968).
- ²⁰Landolt Börnstein, *Nuclear Radii* (Springer-Verlag, Berlin, 1967), Vol. 2.
- ²¹J. P. Schiffer, Nucl. Phys. A335, 339 (1980).
- ²²Y. Ohkubo and L. C. Liu, Phys. Rev. C 30, 254 (1984).
- ²³H. Toki, private communication.
- ²⁴M. Hirata, F. Lenz, and M. Theis, Phys. Rev. C 28, 785 (1983).